Dye-sensitized solar cells based on nanocrystalline TiO_2 films surface treated with Al^{3+} ions: photovoltage and electron transport studies

Hugo Alarcón[1] halarcon@uni.edu.pe, Gerit Boschloo[2], Pablo Mendoza[3], José Solís[1,3] jsolis@ipen.gob.pe, Anders Hagfeldt[2]

[1] Facultad de Ciencias, Universidad Nacional de Ingeniería, P.O. Box 31-139, Lima, Perú
[2] Department of Physical Chemistry, Uppsala University, P.O. Box 579, SE-751 23 Uppsala, Sweden
[3] Instituto Peruano de Energía Nuclear, Av. Canada 1470, Lima 41, Perú

Resumen

Recubrimientos de TiO_2 con la superficie modificada con Al3+ fue fabricada usando una suspensión de TiO_2 con pequeñas cantidades de nitrato de aluminio o cloruro de aluminio sobre sustratos de vidrio conductores, seguido por un proceso de secado, compresión y sinterizado a 530 °C. Los electrodos obtenidos con recubrimientos de nanoparticulas de TiO_2 con menos de 0.3 wt % de oxido de aluminio con respecto al TiO_2 incremente la eficiencia de la celda solar. Esta cantidad corresponde a una monocapa de oxido de aluminio. Entonces, los iones de aluminio terminan la superficie del TiO2 en vez de formar una capa de oxido de aluminio. El ión de aluminio en la superficie afecta la celda solar en diferentes formas: el potencial de la banda de conducción se desplaza, el tiempo de vida media del electrón se incrementa, y el transporte del electrón es lento cuando los iones de aluminio están presentes entre las partículas de TiO_2 interconectadas.

Abstract

Nanocrystalline TiO_2 films, surface modified with Al^{3+}, were manufactured by depositing a TiO_2 suspension containing small amounts of aluminum nitrate or aluminum chloride onto conducting glass substrates, followed by drying, compression, and finally heating to 530 °C. Electrodes prepared with TiO_2 nanoparticles coated with less than 0.3 wt % aluminum oxide with respect to TiO_2 improved the efficiency of the dye sensitized solar cell. This amount corresponds to less than a monolayer of aluminum oxide. Thus, the Al ions terminate the TiO_2 surface rather than form a distinct aluminum oxide layer. The aluminum ion surface treatment affects the solar cell in different ways: the potential of the conduction band is shifted, the electron lifetime is increased, and the electron transport is slower when aluminum ions are present between interconnected TiO_2 particles.

1. Introduction

The dye-sensitized solar cell (DSC) is an interesting alternative solar cell technology that has been intensively studied since the beginning of the 90s [1-3]. A typical DSC comprises a dye-sensitized porous nanostructured TiO_2 film interpenetrated by a liquid electrolyte containing an iodine/iodide redox couple. Recently, a new method was introduced for preparation of nanostructured TiO_2 films at room temperature [4,5]. A TiO_2 powder film is compressed to form a mechanically stable, electrical conducting, porous nanostructured film. Compressed nanostructured TiO_2 films on conducting plastic and glass substrates have been tested for use in DSC. Efficiencies of 4-5% were obtained under simulated solar light illumination [4,5].

In efficient DSC devices the possible recombination pathways occurring at the TiO_2/dye/electrolyte interface should be minimized, allowing charge collection at the device contacts. It has been reported that the DSC's efficiency can be improved by surface modification of TiO_2 by insulating oxides or high band gap semiconductors that form a blocking layer between the dye sensitizer and the semiconductor oxide [6-9]. The electron injection from the excited state of the dye into the conduction band of the TiO_2 can occur by tunneling through the very thin insulating oxide [10]. The thickness of the insulating oxide must be thin enough to allow the passage of electrons by tunneling, otherwise it will decrease the efficiency of the solar cell. The injected electron may recombine at the solid-liquid interface, either with oxidized dye molecules or with the oxidized redox couple. The insulating oxide

layer can reduce the interfacial recombination. There are several methods to deposit ultrathin insulating oxides, such as Nb_2O_5 and Al_2O_3, onto the TiO_2 nanoporous matrix. Dip-coating in metal alkoxide solution, followed by annealing, has been used in several studies [9,10]. Atomic layer chemical vapor deposition has been used by Goossens et al.[11]. A very simple method is to mix metal salts into the TiO_2 suspension, so that a metal oxide coating is formed upon sintering [8]. The advantage of this method is that the amount of insulating metal oxide can be controlled accurately.

This paper presents the efficiency optimization and optoelectrical characterization of dye-sensitized solar cells based on TiO_2 coated with aluminum oxide. Homogeneous aqueous mixtures of TiO_2 powder and different amounts of aluminum chloride or aluminum nitrate were prepared. These mixtures were spread out, allowed to dry, compressed, and finally annealed to oxidize the aluminum salt. The influence of the amount of aluminum oxide deposited on TiO_2 on the solar cell performance, charge transport, and charge recombination was investigated. It is demonstrated that the amount of aluminum oxide affects the energetics and the kinetics of the dye-sensitized solar cell, and thereby its power conversion efficiency. Best results are obtained with aluminum oxide coatings that correspond to much less than monolayer coverage.

2. Experimental Section

2.1 Pressed Films

Nanostructured TiO_2 films coated with aluminum oxide were prepared by the following method. Different amounts of $AlCl_3$ or $Al(NO_3)_3$ were added to an aqueous solution of TiO_2 powder (Degussa P25) to obtain between 0.1 and 3.6 wt % of aluminum oxide in the resulting film. In addition, pure TiO_2 films were prepared as a reference (blank). The suspensions were stirred with a magnetic stirrer for 2 min and agitated ultrasonically for 30 min. The resulting suspension was applied onto a conducting glass substrate (SnO_2: F-coated glass, resistance 8 Ω/square) by doctor blading, using adhesive tape as a frame and spacer. After deposition, the water was allowed to evaporate at room temperature for 2 h. The dry powder film was put between two planar steel press plates and a pressure of 600 kg cm^{-2} was applied by using a hydraulic press [4,5]. The working electrode was annealed in air at 530 °C for 30 min. The mean thickness of the obtained films was around 20 μm, as measured by profilometry (Dektak 3, Veeco Instruments).

The amount of aluminum oxide in the mixture was calculated by assuming that the aluminum salt completely oxidizes during annealing. For example, 12 g of TiO_2 was mixed with 0.05 g of $Al(NO_3)_3$ and 18 g of water (Milli-Q), resulting in 0.012 g of Al_2O_3, which is 0.1 wt % with respect to TiO_2. Using the density of Al_2O_3 (3.97 g/cm^3), the volume of Al_2O_3 is calculated to be 3 x10^{-9} m^3 for this preparation. As the BET average of P25 (TiO_2) is about 55 m^2/g, the thickness of the aluminum oxide layer is therefore estimated to be as low as 5 x10^{-12} m. The coating can therefore not be considered as a complete aluminum oxide shell, but should be seen as a partial surface modification of TiO_2. Using the density of surface titanium atoms of the anatase crystal (Tis ~5.5 x10^{14} cm^{-2}) an Al/Tis ratio or "monolayer coverage" of about 0.04 is calculated for the 0.1 wt % aluminum oxide preparation. The calculated coverage for the different sample preparations is shown in Table 1. About 2.6 wt % of aluminum oxide would be required to obtain a complete monolayer, while 22 wt % is required to obtain a 1 nm thick layer of Al_2O_3 on the TiO_2 nanoparticles.

Table 1: Calculated Monolayer Coverage for Different Aluminum-Modified TiO_2 Preparations and Comparison of the Added and Measured Amount of Aluminum by Neutron Activation Analysis[a]

wt % of aluminum oxide	Al/Tis	Al wt % added	Al wt % measured
0.1	0.04	0.052	0.061
0.6	0.23	0.312	0.380
3.6	1.40	1.872	1.253
0.0	0.00	0.000	0.000

[a] Aluminum was added in the form of $Al(NO_3)_3$.

Surface morphologies were studied by scanning electron microscopy (SEM) using a LEO 1530. An X-ray diffraction study of the samples did not reveal any peaks of crystalline aluminum oxide for the different films. The aluminum oxide coating could be amorphous, or simply too thin to give a significant signal.

The amount of aluminum in the samples was determined by using k_0 based neutron activation analysis [12]. The nanostructured oxide film was scratched from the substrate and weighed (50 mg or 70 mg) and put in polyethylene bags. Sodium pellet (500 μg; 15 mm diameter and 2 mm height) was used as standard. These samples were put together inside polyethylene capsules. The irradiations were carried out for 10 min in the RP-10

reactor of the Instituto Peruano de Energia Nuclear at a thermal flux of 0.5 x10^{12} ncm^2 s^{-1} with use of a pneumatic system. After adequate decay times, the induced radioactivity of the samples and the sodium standard was measured by high-resolution γ-spectrometry with a HP Ge detector, and a source-detector distance of 160 mm [13]. The detector resolution was 1.9 keV for the 1408 keV ^{152}Eu peak. Spectra were acquired with a Canberra GC multichannel analyzer and evaluated with DB Gamma V5.0 software. Elemental concentrations were determined by the k_0 method, using the Högdahl convention [14]. The measured weight percentage of aluminum for films obtained with different amounts of $Al(NO_3)_3$ added to the TiO_2 suspension is shown in Table 1. A good correlation is observed between the amount of aluminum added and measured in the analyzed samples.

2.2 Solar Cell Preparation

The electrodes were dye sensitized by submerging the substrate with the deposited film for 12 h in a dye bath consisting of 0.5 mM *cis*-bis(isothiocyanato)bis-(2,2'bypiridyl-4,4'dicarboxylato) ruthenium(II) bistetrabutylammonium(N719) dye in ethanol. The excess of dye was removed by rinsing the surface of the electrode with ethanol.

The counter electrode was platinized by applying a drop of 5 mM dry H_2PtCl_6 in 2 propanol onto a conducting glass substrate and annealing it in air at 380 °C for 10 min. To fill the cell with the electrolyte a 1 mm hole was drilled in the counter electrode plate. The solar cell was assembled by sandwiching the working and counter electrode using a 60 μm thick thermoplastic frame (Surlyn 1601, Dupont) that melts at around 120 °C. The cell was filled with the electrolyte (0.1 M LiI, 0.6 M tetrabutylammonium iodide, 0.1 M I2, and 0.5 M 4-*tert* butylpyridine in acetonitrile) and the hole was sealed with Surlyn and a cover glass. Silver paint was put on the electrodes to enhance electrical contact with the external circuit. The active area was either 1.5 (Figures 3 and 4) or 0.785 cm2 (Figures 5-7). At least three solar cells were produced at every aluminum salt concentration. The reproducibility was good.

Incident photon-to-current conversion efficiency (IPCE) represents the ratio of the current of the photogenerated electrons to the photon flux irradiating the system. The IPCE was recorded with use of a computerized setup consisting of a xenon arc lamp (300 W Cermax, ILC Technology), a 1/8 m monochromator (CVI Digikröm CM 110), a Keithley 2400 source/meter, and a Newport 1830-C power meter with 818-UV detector head.

The current-voltage (*I-V*) characteristic of the solar cells was monitored and recorded with use of a computerized Keithley 2400 source meter. Sunlight was simulated with a sulfur lamp (Lightdrive 1000 from Fusion Lightning). The calibration versus AM 1.5 was made with a pyranometer (Kipp & Zonen) as described in ref 4. The light intensity during the experiments was 1000 W m^{-2}.

The light source for the electron transport, lifetime, and accumulation studies was a diode laser with variable power and modulation control (Coherent LabLaser, 10 mW, $\ddot{I}$) 635 nm). The beam was expanded to obtain homogeneous illumination of the solar cell. For intensity-modulated photocurrent spectroscopy (IMPS) a sinus modulation with an intensity of about 1% of the total light output was added. The modulated photocurrent was measured by connecting the solar cell to a lock-in amplifier (Stanford Research Systems SR830) via a current amplifier (Stanford Research Systems SR570). Time constants were obtained using a nonlinear least-squares fitting procedure. Photocurrent transients were recorded on a 16-bit resolution data acquisition board (National Instruments). The current was integrated numerically to obtain the charge. The charge recorded in the absence of laser excitation was subtracted to correct for the offset of the instrument. A voltage decaycharge extraction method, similar to that developed by Duffy et al., [15] was used to investigate the relation between charge and potential in the solar cells. The cell was illuminated for 5 s under open-circuit conditions, whereafter the voltage was left to decay for a certain period in the dark (*t*d). Finally, the cell was short-circuited and the current was measured, from which the extracted charge (*Q*) was calculated by integration. A series of measurements was done with *t*d values ranging from 0 to 20 s with a 0.5 s interval.

3. Results

Figure 1 shows a SEM image of a compressed aluminum oxide coated TiO_2 film (3.6 wt % aluminum oxide) on SnO_2:F coated glass. In comparison with an uncoated TiO_2 film (not shown) we observe no specific differences, indicating that the morphology remains unperturbed upon aluminum oxide coating. Similar SEM pictures were obtained for the other aluminum oxide concentrations (0.1% and 0.6%).

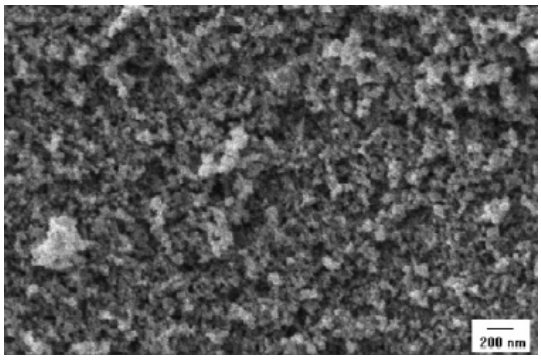

Figure 1. SEM micrograph of a compressed aluminum oxide (3.6 wt. %) modified TiO_2 film.

Figure 2a shows the IPCE as a function of illumination wavelength for cells obtained by using different amounts of $Al(NO_3)_3$ added to the TiO_2 suspension. The film with 0.1 wt % of aluminum oxide shows a maximum IPCE of 0.80 at 550 nm. Higher amounts of aluminum oxide in the film decreased the photoresponse. The film prepared with 0.6 wt % of aluminum oxide has an IPCE of 0.75 at 550 nm whereas the film with 3.6 wt % of aluminum oxide has an IPCE of only 0.35 at the same wavelength. The 0.1 wt % aluminum oxide film has a relatively higher photoresponse for wavelengths longer than 600 nm.

The coloration of all solar cells was approximately equal. Dye-desorption experiments confirmed that the amount of aluminum oxide did not affect the amount of adsorbed dye significantly.
To study the effect of the anion, $AlCl_3$ instead of $Al(NO_3)_3$ salt was added to the TiO_2 suspension. The corresponding IPCE spectra are shown in Figure 2b. Both aluminum salts give a similar behavior in the IPCE values, with the 0.1 wt % aluminum oxide solar cells giving the highest photoresponse. The aluminum nitrate precursor gives better IPCE values than aluminum chloride. In Figure 2c the IPCE spectra for cells with an optimized amount of aluminum oxide (0.1 wt %) and for a blank are compared. It is clearly observed that the measured photocurrent increases with the aluminum oxide treatment.
The current-voltage curves for dye-sensitized solar cells based on TiO_2 with and without 0.1 wt % aluminum oxide using $AlCl_3$ or $Al(NO_3)_3$ are shown in Figure 3. Solar cells with aluminum nitrate additive in the TiO_2 suspension (0.1 wt % aluminum oxide) show the best performance under solar illumination, giving an improvement in current as well as in voltage with respect to the blank.

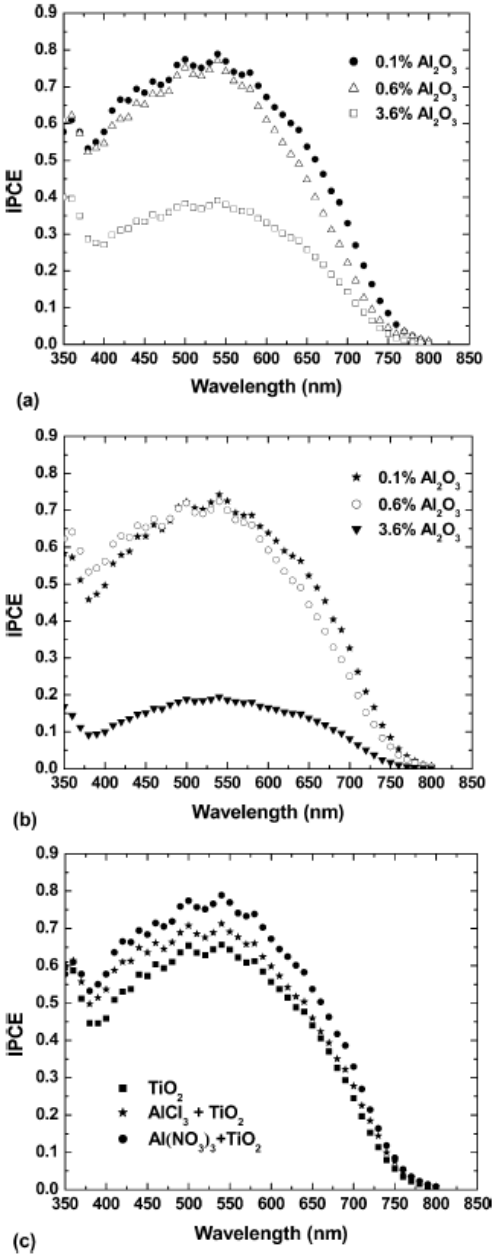

Figure 2. IPCE spectra for samples prepared by adding different amounts of (a) $Al(NO_3)_3$ to the TiO_2 suspension, by adding different amounts of (b) $AlCl_3$ to the TiO_2 suspension. (c) IPCE spectra for the solar cells prepared by adding aluminum salts to the TiO_2 suspension (0.1 wt % aluminum oxide). The photoresponse of an unmodified TiO_2 is also shown as reference.

Figure 4 shows the short circuit current, *I*sc, open circuit voltage, *V*oc, fill factor, FF, and overall efficiency, η, for solar cells with different amounts of aluminum oxide, obtained by adding $AlCl_3$ or $Al(NO_3)_3$ to the TiO_2 suspension.

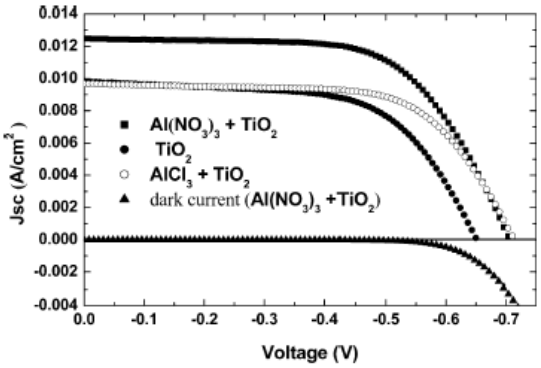

Figure 3. Current-voltage curves of solar cells obtained using pure TiO_2 and by adding $Al(NO_3)_3$ or $AlCl_3$ to the TiO_2 suspension (0.1 wt % of aluminum oxide). The dark current of the $Al(NO_3)_3$ treated TiO_2 film is also shown. The light intensity during the experiments was 1000 W m^{-2}.

The efficiency and the short circuit current show similar trends, i.e., an increase for the cell with a concentration of 0.1 wt % aluminum oxide and a decrease for the cells with concentrations of 0.6 and 3.6 wt %, respectively (Figure 4a). The short circuit photocurrent has a maximum value for cells with 0.1 wt % of aluminum oxide. For cells with higher amount of aluminum oxide the *I*sc decreases strongly (Figure 4b). The open circuit voltage, *V*oc, as well as the fill factor, FF, changes less dramatically as a function of the aluminum oxide content in the films. The *V*oc varies between -0.60 and -0.73 V, whereas the FF changes between 0.56 and 0.63 (Figure 4c,d). The efficiencies of solar cells with pure TiO_2 and TiO_2 modified with 0.1 wt % of aluminum oxide obtained by adding $AlCl_3$ or $Al(NO_3)_3$ are 3.9%, 4.5%, and 5.6%, respectively. Since $Al(NO_3)_3$ gives a better solar cell performance than $AlCl_3$, more detailed experiments were carried out on solar cells prepared with the former salt. Figure 5 shows the results of the combined voltage decay-charge extraction experiments. In Figure 5a the extracted charge (*Q*) is shown as a function of voltage. The 0.1 wt % aluminum oxide solar cell shows a larger amount of charge at a certain voltage compared to the other cells. At a potential of -0.47 V, the charge is around 100 μC cm^{-2} (the area corresponds to the projected electrode area), which corresponds to a concentration of about 6 electrons per TiO_2 particle. For this calculation, it is assumed that the nanoparticles are spherical with a diameter of 25 nm, and that the porosity in the film is 57% [5], so that the number of TiO_2 particles in the film is calculated to be 1.0 x10^{14} cm^{-2}.

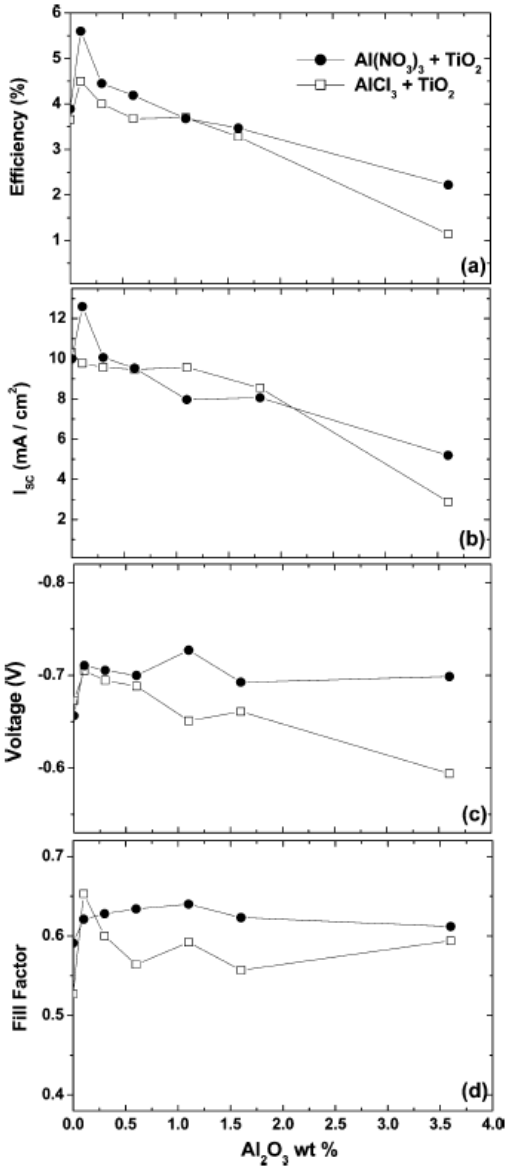

Figure 4. (a) Efficiency, (b) short circuit current, (c) open circuit voltage, and (d) fill factor for solar cells prepared with different amounts of $Al(NO_3)_3$ (●) or $AlCl_3$ (□) to TiO_2. The light intensity during the experiments was 1000 W m^{-2}.

When the charge extraction data are combined with the time delay, the lifetime of the electron (τ_e) can be calculated as follows [16]:

$$\tau_e = Q(t)\left(\frac{dQ(t)}{dt}\right)^{-1} \qquad (1)$$

A (pseudo) first-order recombination reaction for the electrons is assumed in this equation. As the voltage decay takes place in the dark, the resulting lifetime is that of electrons in the dark, which may be longer than that under illumination. Figure 5b shows the lifetime of the electrons as a function of the potential of the dye-sensitized solar cell. The lifetime is

in general quite long (>0.7 s). Aluminum oxide coverage results in longer electron lifetimes at potentials between -0.4 and -0.55 V.

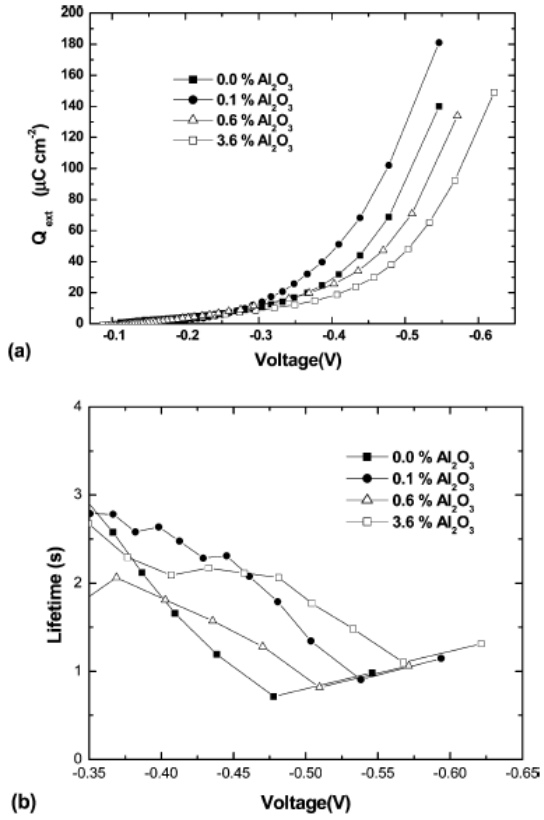

Figure 5. (a) Extracted charge as a function of voltage. (b) Electron lifetime as a function of voltage. The solar cells are prepared with different amounts of $Al(NO_3)_3$.

Electron transport in the aluminum oxide modified TiO_2 solar cells was studied by using intensity-modulated photocurrent spectroscopy (IMPS). The time constants (τ_{IMPS}) that are found are interpreted as transport times, which is a reasonable approximation if the transport time is much smaller than the electron lifetime [17]. Figure 6a shows τ_{IMPS} as a function of light intensity. The electron transport becomes more rapid with increasing light intensity, as has been observed in previous studies [18-20]. The electron transport times are nearly identical for samples without aluminum oxide and with 0.1 wt % aluminum oxide, but increase significantly for samples with more aluminum oxide. The slopes of the curves in the double logarithmic plot are very similar (ca. -0.92).

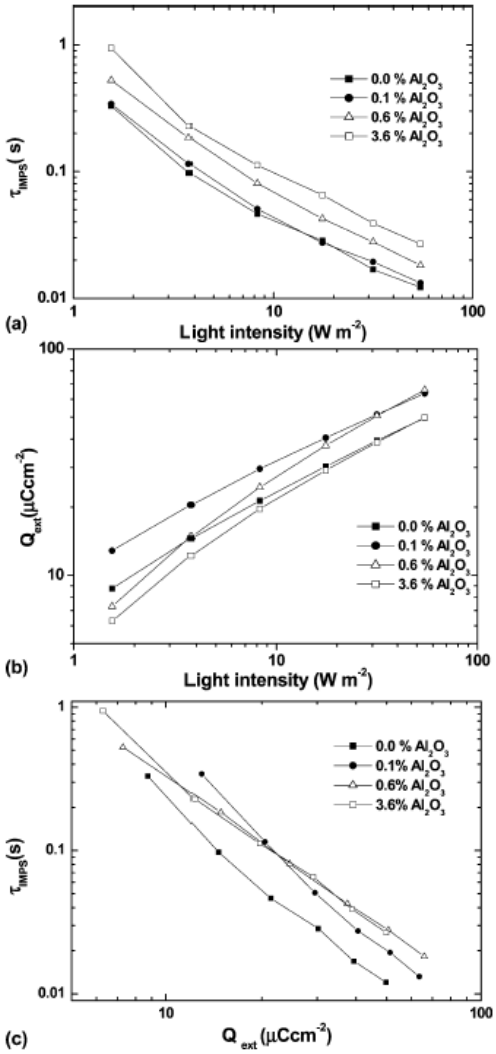

Figure 6. (a) Electron transport time as a function of light intensity, (b) extracted charge as a function of monochromatic light intensity, and (c) electron transport time as a function of extracted charge from the solar cell. The solar cells are prepared with different amounts of $Al(NO_3)_3$.

The transport time of electrons in the nanostructured TiO_2 film is related to the electron concentration in the film. The amount of accumulated electrons was therefore determined by using photocurrent transients. Figure 6b shows the extracted charge under short-circuit conditions as a function of light intensity. The general trend is that the charge in the nanostructured TiO_2 increases with light intensity. The slope in the double logarithmic plot is about 0.43 for all cells. The extracted charge from the solar cell with 0.1 wt % of aluminum oxide is systematically higher than that of the solar cell without aluminum oxide.

Figure 6c shows the electron transport time as a function of the extracted charge. Electron transport becomes faster when more charge is accumulated. Interestingly, all the solar cells treated with aluminum oxide have increased

electron transport times compared to the blank.

4. Discussion

Aluminum salt treatment of TiO_2 affects the solar cell performance in different ways, depending mostly on concentration but to a small extent also on the anion used. $Al(NO_3)_3$ is preferred over $AlCl_3$, as it gives better overall solar cell efficiency. In the following we will only discuss results obtained for $Al(NO_3)_3$. From the concentration dependence of the solar cell efficiency we observed an optimum for very small amounts of aluminum oxide, whereas a decrease in efficiency is observed using higher concentrations. The optimum concentration, 0.1 wt % of aluminum oxide, is so low that it is insufficient to cover the TiO_2 surface completely. It corresponds to only ~4% of full monolayer coverage.
In the following we will rationalize our findings by discussing the effects of the aluminum oxide treatment in terms of band edge movements (energetics), variations in loss reactions, and transport properties (kinetics).

4.1 Effects on Photovoltage

The open-circuit photovoltage (VOC) of the solar cell is given by the difference of the quasi-Fermi level of the electrons in the metal oxide and the potential of the counter electrode, which is equal to the redox potential of the electrolyte. The quasi-Fermi level depends on the accumulated charge in the semiconductor and will approach the conduction band edge when the concentration of conduction band electrons is high. The potential of the conduction band edge (VCB) depends in general on the surface charge of the metal oxide. Since Al_2O_3 is a more basic oxide than TiO_2, we can expect a negative shift of VCB, in the case of aluminum oxide surface modification [10].
The following relation is valid:

$$V_{OC} = V_{CB} - \frac{kT}{e} \ln\left(\frac{n_C}{N_C}\right) \qquad (2)$$

where kT is the thermal energy, e is the elementary charge, n_C is the concentration of electrons in the conduction band, and N_C is the effective density of states in the conduction band. Note that both V_{OC} and V_{CB} are given here with respect to the redox potential of the electrolyte and have negative values.

In Figure 5a open-circuit potentials of aluminum oxide modified TiO_2 solar cells are correlated with the charge present in the nanostructured metal oxide film. This gives a clear indication of shifts of V_{CB} as a function of the aluminum oxide concentration. For 0.6% and 3.6% aluminum oxide V_{CB} is shifted in the negative direction compared to the blank as was expected from the basic nature of aluminum oxide. There is, however, a surprising positive shift of V_{CB} for 0.1% aluminum oxide compared to the standard TiO_2 film. Adsorption of aluminum ions will result in a more positive charge at the TiO_2 electrolyte interface and a positive shift of V_{CB}. During heat treatment, however, one would expect a conversion to aluminum oxide, giving a negative shift instead. Apparently, some of the ion adsorption effect is maintained after the heat treatment.

Considering the positive shift of V_{CB} for the 0.1% aluminum oxide solar cell one might expect a decrease in V_{OC} with respect to the blank in the current-voltage characterization (Figures 3 and 4). This is, however, not the case. From Figure 4 it follows that VOC is slightly more negative for the 0.1% solar cell than for the blank. The reason must be a higher n_C due to either a better injection of electrons into the metal oxide from the excited dye or suppression of loss reactions. An investigation of the injection process was beyond the scope of this work. Regarding loss reactions, Figure 5b shows measurements of the lifetime of electrons in the oxide film as a function of voltage. It is clearly observed that the aluminum oxide treatments have a beneficial effect, giving generally higher electron lifetimes. In particular, we note that the lifetime of the electrons is improved at the working point of the solar cell, which is at about -0.43 V as obtained from Figure 3. As the aluminum oxide content appears to be too small to form a blocking layer, specific suppression of recombination centers by the aluminum ions seems the most likely explanation for this effect.
The negative shift of V_{CB} of the 0.6 and 3.6 wt % aluminum oxide solar cells that follows from Figure 5a is translated into a more negative V_{OC} in the current-voltage curves compared to the blank for the 0.6% cell but not for the 3.6% cell. A possible cause is a reduced electron injection in the 3.6% cell, as will be discussed in more detail below.

4.2 Effects on Photocurrent

The overall photocurrent can besides being measured in a solar simulator also be calculated by multiplying the IPCE values with the number of photons at a given wavelength under AM 1.5 solar conditions and integrating over the entire spectrum. In our analysis of the effect of aluminum ion surface treatment on the photocurrent we

therefore use IPCE data for the discussion. The IPCE values can be rationalized by the following relationship [21]:

$$IPCE(\lambda) = LHE(\lambda) x \phi_{inj} x \eta_C \quad (3)$$

where LHE(λ) is the light harvesting efficiency, ϕ_{inj} is the quantum yield of electron injection from excited dye molecules into the semiconductor conduction band, and η_C is the efficiency of collecting the injected charge at the back contact.

Differences in LHE are not expected to be significant in the presented experiments since nanostructured films of equal thickness were used and since the aluminum modification did not affect dye uptake. In Figure 2c an increase of the IPCE values upon aluminum oxide treatment (0.1%) is observed. This can be explained by an improved injection efficiency since there appears to be a positive shift of the V_{CB} by the aluminum ion treatment, Figure 5a, resulting in an improved overlap of excited dye orbitals with conduction band acceptor levels. Furthermore, Figure 5b shows that the aluminum oxide treatment results in longer electron lifetimes, indicating a reduction of loss reactions and a probable increase of the charge collection efficiency.

Comparing the IPCE values as a function of aluminum oxide concentration we note a large decrease in IPCE for the 3.6 wt % sample, see Figure 2a. This is most likely caused by a decrease in the injection efficiency for the thicker aluminum oxide layer. A careful examination of parts a and b of Figure 2 shows a blue shift of the IPCE spectra for the 0.6% aluminum oxide concentration with respect to the 0.1% samples. This finding seems to confirm the shifts of V_{CB} as discussed above. A negative shift of V_{CB} can lead to a decrease in injection efficiency when the dye is excited with lower energy photons. A similar effect was discussed in detail by Boschloo et al.[22], who observed a negative shift of V_{CB} upon addition of 4-*tert*butylpyridine to the electrolyte.

The transport of electrons in the nanostructured TiO_2 electrode is affected by the aluminum oxide modification, see Figure 6. The general trends are similar in the investigated solar cells: The transport time decreases and the accumulated charge in the nanostructured electrode increases with increasing light intensity. It should be noted that a certain light intensity results in different fluxes of photoinjected electrons and short-circuit photocurrents, depending on the amount of aluminum oxide present. For a proper comparison of electron transport in the aluminum oxide modified TiO_2 films, it is therefore convenient to relate the electron transport times to the amount of accumulated charge present in the nanostructured film. This relation is shown in Figure 6c. The effect of the aluminum oxide can be clearly observed in this figure: addition of aluminum oxide increases τ_{IMPS}. A possible explanation is that aluminum ions will be present at the grain boundaries between TiO_2 particles. This may result in the formation of a barrier for electron transport, as is indicated in Scheme 1a.

Scheme 1: Schematic Representation of Aluminum Oxide Coated TiO_2 Nanoporous Films[a]

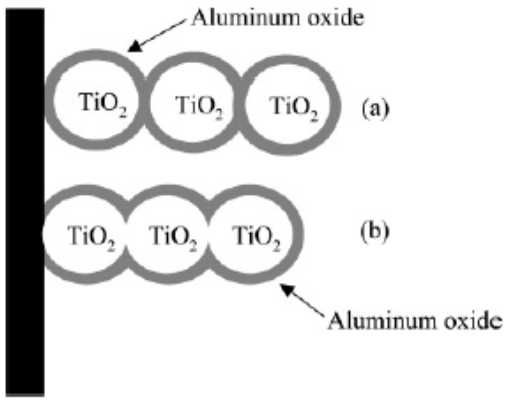

[a] Note that the coating is not continuous in our study: (a) prepared from a suspension of TiO_2 particles and dissolved $Al(NO_3)_3$ followed by compression and sintering; (b) coating is made on a compressed TiO_2 film.

To test this hypothesis, an additional series of solar cells was made. A comparison was made between cells where (1) the $Al(NO_3)_3$ was mixed with a suspension of TiO_2 particles followed by pressing and sintering as before and (2) a pressed and sintered TiO2 film was treated with a precise amount of $Al(NO_3)_3$ in ethanol, corresponding to 0.1wt % aluminum oxide as in the first experiment, followed by another heat treatment. The latter treatment avoids the presence of aluminum atoms at grain boundaries between the TiO_2 particles, as shown schematically in Scheme 1b.

The results of transport and charge extraction measurements of this comparison are shown in Figure 7. No significant differences in τ_{IMPS} were found as a function of light intensity (Figure 7a). There are, however, more electrons accumulated under short-circuit conditions in the solar cell where the TiO_2 and $Al(NO_3)_3$ were mixed (Figure 7b).

From the plot of τ_{IMPS} vs extracted charge (Figure 7c) it follows that the electron transport is unaffected by the aftertreatment of the nanoporous TiO_2 film with aluminum nitrate, whereas mixing of the aluminum salt with the TiO_2 suspension leads to a reduction of the electron transport speed. Considering the very small amounts of aluminum ions used in these experiments the results should be interpreted with care, but they seem to confirm our hypothesis that aluminum ions present between TiO_2 particles reduce the electron transport speed due to formation of an energy barrier.

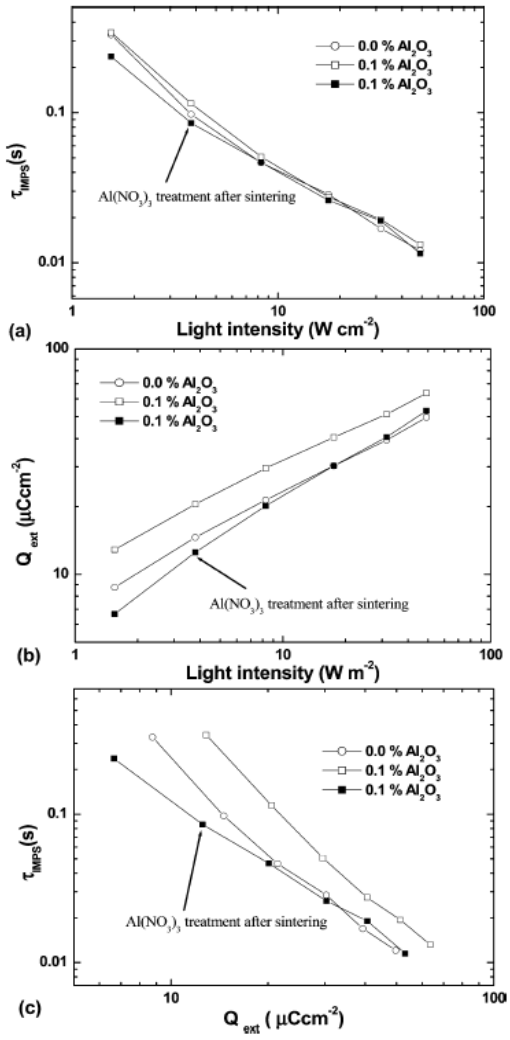

Figure 7. Comparison between solar cells: (1) prepared from a suspension of TiO_2 particles and dissolved $Al(NO_3)_3$ followed by compression and sintering, with 0.0 wt % of aluminum oxide (○) or 0.1 wt % of aluminum oxide (□), (2) a coating of $Al(NO_3)_3$ is made on a compressed TiO_2 film, followed by heating, corresponding to 0.1 wt % of aluminum oxide (■). (a) Electron transport time as a function of light intensity, (b) extracted charge as a function of light intensity, and (c) electron transport time as a function of extracted charge from the solar cell.

The relatively slow and light-intensity dependent electron transport in nanostructured TiO_2 electrodes is most often explained by using a trapping/detrapping model [18-20]. Traps are localized states with energies below the conduction band edge and located either in the bulk of the semiconductor material or at the semiconductor/electrolyte interface. Electrons can be captured (trapping) and released after some time by thermal excitation (detrapping). The power-law dependence of the electron transport time and the extracted charge on light intensity can be explained by assuming a trap distribution that increases exponentially toward the conduction band [19,20]. The slope of the trap distribution can be determined from the double logarithmic plots of τ_{IMPS} and extracted charge vs light intensity (Figure 6a,b). It follows from this figure that this slope does not change significantly with aluminum oxide coverage. This may be an indication that traps are not located at the semiconductor/electrolyte interface where aluminum ion treatment is expected to have a large effect. It also appears that the aluminum salt treatment does not create a large amount of additional trap states, as the charge in the film remains quite similar (Figure 6b).

4.3 Comparison with Other Studies

$Al(NO_3)_3$, as well as $Mg(NO_3)_2$ and $Y(NO_3)_3$, were used by Kay and Grätze [l8] to surface-modify TiO_2 in a similar way as in this study. A reasonable result was obtained with a coverage corresponding to 0.05 nm of Al2O3, giving higher V_{OC} but lower I_{SC} than the blank, and a slight reduction in overall efficiency. This coverage would be equivalent to 1.0 wt % of Al_2O_3 in our study, and a comparison shows that their result is in accordance with the trends that we find.

In the work of Palomares et al. [10] aluminum oxide surface-modification of TiO_2 was achieved by hydrolysis of an aluminum alkoxy precursor. The Al_2O_3 coating thickness was estimated to be 0.9 nm from HRTEM and XPS studies. This is about 5 times thicker than the estimated thickness in our 3.6 wt % preparation. V_{OC}, I_{SC}, and overall efficiency were found to be improved with respect to the blank, a situation that we only found in the 0.1 wt % preparation in our study. Although the preparation methods differ, it is surprising to see that the coating thickness dependence would be so different. The fact that Palomares et al. did not observe a decrease in the porosity after the coating procedure may suggest that their coating is thinner than reported. They found that the aluminum oxide coating retards the

interfacial recombination between electrons in the TiO_2 and oxidized dye molecules. Similarly, we have shown that the recombination between electrons and triiodide is slowed down upon aluminum ion surface modification.

5. Summary and Concluding Remarks

Dye-sensitized TiO_2 solar cells prepared by using the compression method and surface modified with aluminum ions can have a significantly improved solar cell efficiency compared to unmodified TiO_2 films. The best performance was obtained with titanium dioxide films modified with 0.1 wt % of aluminum oxide, using aluminum nitrate. Higher concentrations of aluminum oxide reduced the solar cell performance. At this concentration the density of aluminum atoms at the oxide surface corresponds to only ~4% of the surface density of titanium atoms.

The effects of aluminum ion treatment are shifts of the potential of the conduction band, improvement of the electron lifetime, and slower electron transport when the aluminum oxide coating is located between interconnected TiO_2 particles. As no additional trap states were induced by the aluminum ion treatment, the reduced transport is attributed to formation of energy barriers at the grain boundaries between TiO_2 particles.

6. Acknowledgment

H.A. wants to thank the International Science Program in the Chemical Sciences at Uppsala University for a scholarship. The Swedish Energy Agency, the Swedish Foundation for Strategic Environmental Research (MISTRA), and PSO project 3629 (Denmark) are gratefully acknowledged for financial support.

7. References

[1] O'Regan, B.; Grätzel, M. *Nature* **1991**, *353*, 737.
[2] Hagfeldt, A.; Grätzel, M. *Chem. Rev*. **1995**, *95*, 49.
[3] Hagfeldt, A.; Grätzel, M. *Acc. Chem. Res.* **2000**, *33*, 269.
[4] Lindstro¨m, H.; Holmberg, A.; Magnusson, E.; Lindquist, S.-E.; Malmqvist, L.; Hagfeldt, A. *Nano Lett*. **2001**, *1*, 97.
[5] Lindstro¨m, H.; Holmberg, A.; Magnusson, E.; Malmqvist, L.; Hagfeldt, A. *J. Photochem. Photobiol. A*: *Chem*. **2001**, *145*, 107.
[6] Tennakone, K.; Kottegoda, I. R. M.; De Silva, L. A. A.; Perera, V. P. S. *Semicond. Sci. Technol*. **1999**, *14*, 975.
[7] Kumara, G. R. R. A.; Tennakone, K.; Perera, V. P. S.; Konno, A.; Kaneko, S.; Okuya, M. *J. Phys. D*: *Appl. Phys*. **2001**, *34*, 868.
[8] Kay, A.; Grätzel, M. *Chem. Mater*. **2002**, *14*, 2930.
[9] Zaban, A.; Chen, S. G.; Cappel, S.; Gregg, B. A. *Chem. Commun*. **2000**, 2231.
[10] Palomares E.; Clifford, J. N.; Haque, S. A.; Luz, T.; Durrant, J. R. *J. Am. Chem. Soc*. **2003**, *125*, 475.
[11] Nanu, M.; Schoonman, J.; Goossens, A. *Adv. Mater*. **2004**, *16* (5),453.
[12] De Corte, F. Habilitation Thesis, Ghent University, Faculty of Sciences, Belgium, 1987.
[13] Montoya, E. H.; Cohen, I. M.; Mendoza, P.; Torres, B.; Bedregal, P. *J. Radioanal. Nucl. Chem*. **1999**, *240*, 475.
[14] Högdahl In *Radiochemical Methods of Analysis*: IAEA: Vienna. 1965; Vol. 1, p 23.
[15] Duffy, N. W.; Peter, L. M.; Rajapakse, R. M. G.; Wijayantha, K. G. U. *Electrochem. Commun*. **2000**, *2*, 658.
[16] Boschloo, G.; Hagfeldt A. *J. Phys. Chem. B* **2005**, *109*, 12093-12098.
[17] van de Lagemaat, J.; Park, N.-G.; Frank, A. J. *J. Phys. Chem. B* **2000**, *104*, 2044.
[18] Dloczik, L.; Ileperuma, O.; Lauermann, I.; Peter, L.; Ponomarev, E.; Redmond, G.; Shaw, N.; Uhlendorf, I. *J. Phys. Chem. B* **1997**,*101*, 10281.
[19] van de Lagemaat, J.; Frank, A. J. *J. Phys. Chem. B* **2000**, *104*, 4292.
[20] Fisher, A. C.; Peter, L. M.; Ponomarev, E. A.; Walker, A. B.; Wijayantha, K. G. U. *J. Phys. Chem. B* **2000**, *104*, 949.
[21] Nazeeruddin, M. K.; Kay, A.; Rodicio, I.; Humpry-Baker, R.; Muller, E.; Liska, P.; Vlachopoulos, N.; Gratzel, M. *J. Am. Chem. Soc.* **1993**, *115*, 6382.
[22] Boschloo, G.; Lindström, H.; Magnusson, E.; Holmberg, A.; Hagfeldt, A. *J. Photochem. Photobiol. A*: *Chem*. **2002**, *148*, 11.